Scanning tunnelling microscopy and spectroscopy of nanocrystalline silicon films

2001 Semicond. Sci. Technol. 16 789

(http://iopscience.iop.org/0268-1242/16/9/309)

INSTITUTE OF PHYSICS PUBLISHING SEMICONDUCTOR SCIENCE AND TECHNOLOGY
Semicond. Sci. Technol. **16** (2001) 789–792 PII: S0268-1242(01)23705-5

Scanning tunnelling microscopy and spectroscopy of nanocrystalline silicon films

E Nogales[1], B Méndez[1], J Piqueras[1] and R Plugaru[2]

[1] Departamento de Física de Materiales, Facultad de Físicas, Universidad Complutense, E-28040 Madrid, Spain
[2] Institute of Microtechnology, Str. Erou Iancu Nicolae 32B, Sector 2, 72996 Bucharest, Romania

E-mail: bianchi@eucmos.sim.ucm.es

Received 6 April 2001
Published 9 August 2001
Online at stacks.iop.org/SST/16/789

Abstract
Scanning tunnelling microscopy (STM) has been sometimes applied in recent years to characterize porous silicon. In contrast, other forms of light emitting Si, such as nanocrystalline silicon films, prepared by different methods, have not been, or are only occasionally, studied by STM related techniques. In this paper STM and spectroscopy measurements have been performed on nanocrystalline silicon films obtained by low pressure chemical vapour deposition followed by boron implantation. Subsequent annealing of the samples caused an increase of the crystallites size. Scanning tunnelling spectroscopy enabled us to determine the surface band gap in films. In all annealed nanocrystalline films the value of this gap is similar to the value in bulk Si. However, a large value of the gap, of about 4.5 eV, is measured in as-implanted films. The different behaviour is explained in terms of a quantum confinement effect related to the nanocrystal's size.

1. Introduction

Studies of the structure and properties of nanocrystalline silicon (nc-Si) have increased during the past decade because of its potential application in optoelectronic devices. In particular, porous silicon, which shows visible emission at room temperature, has been widely investigated and many of the experimental results have been explained in the framework of a quantum confinement model (for a review see [1]). Other forms of luminescent nc-Si have attracted considerable attention in recent years because of their stability and potential high compatibility with integrated circuits. This is the case of silicon nanocrystals formed by Si ion implantation into an oxide layer [2,3] and of nc-Si films prepared by crystallization of amorphous silicon [4]. Although the visible luminescence of different forms of nc-Si is basically explained by quantum confinement effects, the influence of states at the surface of the nanocrystals or at the interface between the nanocrystals and oxides or amorphous phases has to be considered to interpret the results [5–8]. Scanning tunnelling microscopy (STM) has been sometimes used to characterize the surface of nc-porous silicon, providing information on the topography and on the local luminescence behaviour of the crystallites [9–11]. In addition, scanning tunnelling spectroscopy (STS) has been applied [12–15] to investigate electronic properties as I–V characteristics and local surface density of states of porous silicon. However, the porous silicon results cannot be extrapolated to the case of nc-Si films whose surface structure and properties are often different.

In this paper we study the surface of nc-Si films grown by low pressure chemical vapour deposition (LPCVD) followed by boron ion implantation using STM and STS. In particular, STS has been applied to study the surface density of states and the surface band gap values of samples after different implantation and annealing treatments. The nc-Si films used have been previously found to show visible luminescence with the main emission at about 3 eV [16, 17].

2. Experiment

Amorphous silicon films with a thickness of about 2 μm were obtained by LPCVD on p-type (100) silicon wafers at

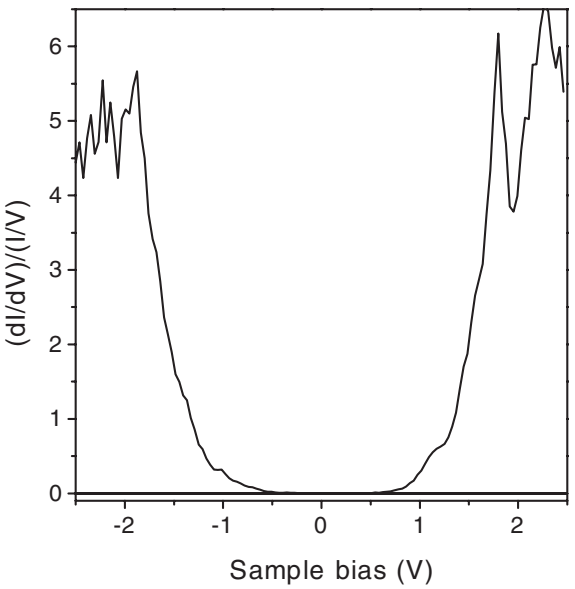

Figure 1. Normalized differential conductance curve of the reference Si wafer. A band gap value of about 1.1 eV is measured.

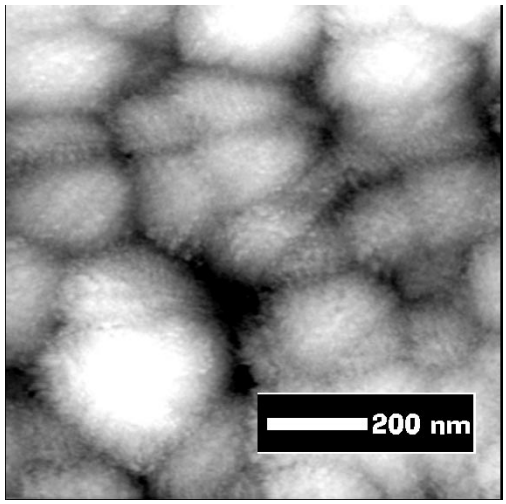

Figure 2. Representative constant-current STM image of B-implanted Si. The sample bias was +2.5 V and the tunnelling current 0.15 nA.

a temperature of 570 °C and a pressure of 0.4 Torr. Some of the films were implanted with boron ions with an energy of 100 keV and doses of 10^{14} or 10^{15} cm^{-2}. As-deposited as well as implanted films were annealed at 650 °C for 1 h. A piece of Si wafer was used as a reference sample for the STM measurements. The structure of the films was investigated by x-ray diffraction (XRD) techniques. For the STM measurements the samples were prepared according to the procedure described in [18]. They were cleaned following the standard RCA cleaning procedure and then were dipped into a dilute HF solution to remove the surface oxide and provide an unpinned hydrogen terminated surface. Finally the samples were rinsed in de-ionized water and blown dry with nitrogen. The microscopic measurements were performed in a combined scanning electron microscope (SEM)–STM system based on a Leica 440 SEM operating under a vacuum of 1×10^{-6} Torr [19, 20]. Mechanically sharpened Pt–Ir wires were used as probe tips. The STM was used in the conventional constant-current mode and in the STS mode. The STS mode [21] provides information on surface electronic states by recording I–V curves at fixed tip–sample separation. The obtained I–V curves at every point depend, through the tunnelling current, on both tip–sample separation and applied bias voltage. Most of this dependence can be removed [21] by plotting the ratio of differential to total conductance, $(\mathrm{d}I/\mathrm{d}V)/(I/V)$, which provides a rather direct measure of the surface density of states [22].

3. Results and discussion

XRD showed an amorphous structure in the as-deposited films. After implantation, crystallites with ⟨111⟩⟨220⟩ and ⟨211⟩ orientations were revealed by XRD. The average grain size for the ⟨211⟩ orientation was estimated to be about 8 nm and somewhat higher for other orientations. It has been previously observed [23] that implantation at lower doses (10^{13} cm^{-2}) causes the appearance of crystallites with ⟨111⟩ and ⟨220⟩ textures with 8 nm grain size. Increasing the dose to the values used here induces the new ⟨211⟩ orientation and the size increase of the grains with other orientations. Annealing the implanted samples produces, independent of the implantation dose, the grain size increase to average values of about 9–11 nm. In the unimplanted films the final grain size after annealing is about 16 nm.

The reference sample was a piece of Si wafer used as substrate for the LPCVD films, with a resistivity of about 12–18 Ω cm. This resistivity is close to that of the samples used by Lin *et al* [18] in a study of the suitable conditions to measure the energy gap in lightly doped silicon by STS. These authors demonstrated that, with the above described RCA modified cleaning procedure and the use of Pt–Ir tips, a gap of 1.1 eV is measured and that the spectral shifts due to tip induced band bending are eliminated. Figure 1 shows the normalized differential conductance curve of the Si wafer used in this paper. The gap of about 1 eV shows good agreement with the value obtained in [18] and indicates that the experimental conditions used here are appropriate for STS measurements of Si with low carrier concentration.

The as-deposited amorphous films are too resistive to be investigated with the STM. In the as-implanted samples, tunnel current was unstable during imaging recording, which is attributed to the resistivity of the sample, and stability increased in the case of annealed samples. Constant-current STM images of the samples show a cell structure, with cell dimension, depending on the sample and area considered, of about one or several tenths of a micron, as figure 2, that corresponds to an as-implanted film, shows. This structure is also revealed in the implanted films by atomic force microscopy [23]. The nanocrystals can be observed within the cells at higher magnification. This is shown for the annealed samples in figure 3. The as-implanted samples present a similar, but more unstable, appearance with a somewhat smaller nanocrystal size. Images of the nanocrystals were used to locate different points to perform the conductance measurements. Normally the tip was located at the centre of the region corresponding to a nanocrystal as shown in figure 3.

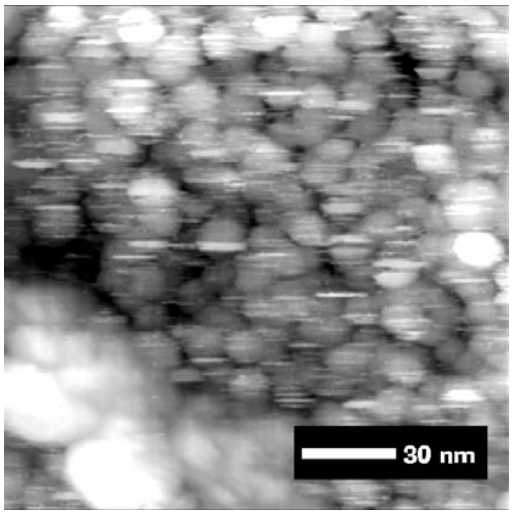

Figure 3. Constant-current STM image of a detail of the grain structure within the cells. The sample bias was +2.5 V and the tunnelling current 0.05 nA.

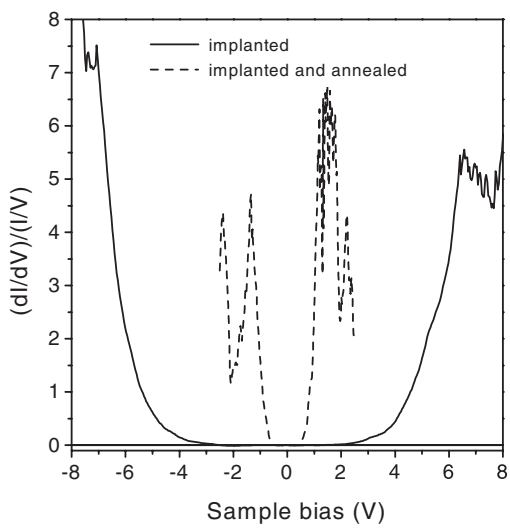

Figure 4. Representative normalized differential conductance curves of the samples used in this paper. The full curve corresponds to 10^{14} cm^{-2} B implanted film. The broken curve corresponds to the same film after a 1 h 650 °C annealing.

After implantation with the two doses used, the conductance curves of the films always show a wider band gap than the wafer. Figure 4 shows one representative curve of the as-implanted samples with a band gap of about 4.5 eV. However, fluctuations of a few tenths of eV from this value have been observed. After annealing at 650 °C, the as-deposited and all the implanted samples present a conductance behaviour similar to that of the single-crystalline wafer. In figure 4 the curve of one implanted and subsequently annealed sample, representative of the behaviour of all samples after annealing, can be compared with the curve of the same sample after implantation.

The present results show that the STS curves of the single-crystalline wafer and of all nanocrystalline structures obtained after the annealing treatment are comparable and show a band gap close to the bulk value. No quantum confinement effect is detected in these samples which is explained by their large average grain size, as measured by STM (figure 3) and XRD, and the associated reduced fraction of the amorphous phase. The normalized differential conductance curves show that the gap in the implanted samples is considerably larger. These samples have nanocrystals with a smaller size and quantum confinement effects would influence the conductance curves. This effect is influenced by the fact that the nanocrystals are formed by recrystallization in an amorphous matrix and cannot be directly compared with the case of hydrogen terminated nanocrystals reported in the literature. Nomura *et al* [24] have studied the electronic structure of a model nanocrystalline phase/amorphous phase silicon and calculated the local density of states in the nanocrystalline phase. Their results, which correspond to a model structure with fixed dimensions of the nanocrystals and the amorphous surrounding layer, show a distribution of the density of states involving optical transitions, mainly of energies of about 3–4 eV, which is of the order of the gap, of about 4.5 eV, detected here by STS. In [4, 7] such energies were also measured in photoluminescence experiments on nanocrystalline films containing 3–5 nm size crystallites in an amorphous matrix.

It is pointed out that the surface gap value measured from the conductance curves is affected by some factors and could not correspond to the real surface band gap. One possible factor in the implanted samples, that are more resistive than the annealed ones, is the surface band bending that could lead to an overestimated band gap [25]. McEllistrem *et al* [26] considered that the effect of the tip–sample interaction cannot be readily predicted nor can it be measured using conventional STS techniques, and they measured the tip induced band bending by surface photovoltage techniques. The values obtained correspond to a small fraction of the gaps measured here by STS. The results of [25] for different III–V materials provide spectral shifts due to tip-induced band bending of a few tenths of an eV or smaller.

The different conductance behaviour of samples with small size nanocrystals, as compared with single crystals or samples with larger nanocrystals, is attributed to the quantum confinement. The influence of the implantation on the resistivity of the films does not explain the high band gap of the as-implanted samples and its reduction after annealing. This is observed by the fact that samples implanted with two different doses present the same conductance spectra and that the conductance behaviour similar to that of the bulk silicon is reached after annealing at 650 °C. Previous works on implanted polysilicon layers [27,28] showed that, for implantation doses similar to those used here, even after annealings at temperatures of 1100 or 900 °C the resistivity of the films is higher than 10^4 Ω cm. In this paper annealing at the lower temperature of 650 °C cannot reduce the implantation induced resistivity.

It does not appear that the curves enable us to correlate the size of the nanocrystals with band gap energy from the point of view of a pure quantum confinement model. However, the values obtained by STS are comparable to theoretical calculations in nanocrystaline/amorphous mixed-phase silicon. Surface and interface states, or the band bending discussed above, possibly influence the gap measured by STS. In fact previous tunnelling conductance measurements in nanocrystalline porous silicon [12] did not reveal an increased band gap related to the nanocrystals. The authors tentatively

explained their observation by a high background density of states due to surface material. Yu *et al* [13] obtained normalized conductance curves of porous silicon by applying only positive bias voltage to the tip. They observed an increase of the density of states above 2 eV and associated this value with the band gap of quantum wires. This value is comparable to that shown in figure 4 for positive bias. Our results include both positive and negative bias and the gap measured is markedly higher than that reported in [13]. The present results cannot be related to the previous luminescence measurements [16, 17] on these samples showing emission bands that do not correspond to transitions across the gaps measured in this paper. Similar lack of concordancy between density of states spectra and luminescence emission have been reported in [12].

4. Conclusions

In summary, STM and spectroscopy measurements of nc-Si films have been presented. The films were obtained through boron implantation, with different doses, on amorphous layers and were imaged by STM. Normalized differential conductance curves from all the as-implanted layers show a surface band gap value of 4.5 eV. The nanocrystalline layers after annealing at 650 °C, as well as an untreated reference wafer, showed a band gap value of about 1 eV. The difference observed is mainly attributed to quantum confinement effects in the as-implanted layer. The larger average nanocrystal size, shown by STM images and XRD techniques, after annealing explains the conductance behaviour of the thermally treated samples similar to that of the bulk silicon.

Acknowledgments

This work was supported by DGES (PB96-0639) and by the Scientific Cooperation Program between Spain and Romania.

References

[1] Cullis A G, Canham L T and Calcott P D 1997 *J. Appl. Phys.* **82** 909
[2] Shimizu-Iwayama T, Nakao S and Saitoh K 1994 *Appl. Phys. Lett.* **65** 1814
[3] Mutti P, Ghislotti G, Bertoni S, Bonoldi L, Gerofolini G F, Meda L, Grilli E and Guzzi M 1995 *Appl. Phys. Lett.* **66** 851
[4] Zhao X, Schoenfeld O, Kusano J, Aoyagi Y and Sugano T 1994 *Japan. J. Appl. Phys.* **33** L649
[5] Kanemitsu Y 1994 *Phys. Rev.* B **49** 16845
[6] Shimizu-Iwayama T, Kurumado N, Hole D E and Townsend P D 1998 *J. Appl. Phys.* **83** 6018
[7] Zhao X, Nomura S, Aoyagi Y and Sugano T 1996 *J. Non-Cryst. Solids* **198–200** 847
[8] Wolkin M V, Jorne J, Fauchet P M, Allan G and Delerue C 1999 *Phys. Rev. Lett.* **82** 197
[9] Dumas Ph, Gu M, Syrykh C, Gimzewski J K, Makarenko I, Halimaui A and Salvan F 1993 *Europhys. Lett.* **23** 197
[10] Dumas Ph, Gu M, Syrykh C, Halimaui A, Salvan F, Gimzewski J K and Schlitter R R 1994 *J. Vac. Sci. Technol.* B **12** 2064
[11] Ito K, Ohyama S, Uehara Y and Ushioda S 1995 *Appl. Phys. Lett.* **67** 2536
[12] Amisola G B, Behrensmeier R, Galligan J M, Otter F A, Namavar F and Kalkhoran N M 1992 *Appl. Phys. Lett.* **61** 2595
[13] Yu T, Laiho R and Heikkilä L 1994 *J. Vac. Sci. Technol.* B **12** 2437
[14] Pavlov A and Pavlova Y 1997 *Thin Solid Films* **297** 132
[15] Laiho R, Pavlov A and Pavlova Y 1997 *Thin Solid Films* **297** 138
[16] Méndez B, Piqueras J, Plugaru R, Craciun G, Nastase N, Cremades A and Nogales E 1998 *Solid State Phenom.* **63–64** 191
[17] Piqueras J, Méndez B, Plugaru R, Craciun G, García J A and Remón A 1999 *Appl. Phys.* A **68** 329
[18] Lin H A, Jaccodine R and Freund M S 1998 *Appl. Phys. Lett.* **72** 1993
[19] Panin G, Díaz-Guerra C and Piqueras J 1998 *Appl. Phys. Lett.* **72** 2129
[20] Hidalgo P, Méndez B, Piqueras J, Dutta P S and Dieguez E 1999 *Phys. Rev.* B **60** 10613
[21] Stroscio J A, Feenstra R M and Fein A P 1986 *Phys. Rev. Lett.* **57** 2579
[22] Feenstra R M, Stroscio J A and Fein A P 1987 *Surf. Sci.* **181** 295
[23] Plugaru R, Piqueras J, Méndez B, Craciun G and Nastase N 1999 *Mater. Res. Soc. Symp. Proc.* **536** 63
[24] Nomura S, Zhao X, Aoyagi Y and Sugano T 1996 *Phys. Rev.* B **54** 13974
[25] Feenstra R M 1994 *Phys. Rev.* B **50** 4561
[26] McEllistren M, Haase G, Chen D and Hammers R J 1993 *Phys. Rev. Lett.* **70** 2471
[27] Seto J Y W 1975 *J. Appl. Phys.* **46** 5247
[28] Lee E G and Im H B 1991 *J. Electrochem. Soc.* **138** 3465